Selective laser melting of Inconel 718 under high laser power

Borisov, E. V.; Popovich, V. A.; Popovich, A. A.; Sufiiarov, V. Sh; Zhu, Jia Ning; Starikov, K. A.

DOI
10.1016/j.matpr.2020.01.571

Publication date
2020

Document Version
Final published version

Published in
Materials Today: Proceedings

Materials Today: Proceedings 30 (2020) 784–788

Contents lists available at ScienceDirect

Materials Today: Proceedings

journal homepage: www.elsevier.com/locate/matpr

Selective laser melting of Inconel 718 under high laser power

E.V. Borisov [a,*], V.A. Popovich [b], A.A. Popovich [a], V.Sh. Sufiiarov [a], Jia-Ning Zhu [b], K.A. Starikov [a]

[a] Peter the Great St.Petersburg Polytechnic University, Saint-Petersburg, Russia
[b] Delft University of Technology, Department of Materials Science and Engineering, Delft, The Netherlands

ARTICLE INFO

Article history:
Received 8 December 2019
Accepted 29 January 2020
Available online 19 February 2020

Keywords:
Additive manufacturing
Selective laser melting
Nickel alloy
Grain structure
Texture

ABSTRACT

Selective laser melting (SLM) process has been lately extensively applied in manufacturing of Nickel-based super alloys, which compared to conventional manufacturing routes offers increased design flexibility and simplification of the manufacturing process. However, in order to make SLM process even more beneficial, its process time has to be reduced. One of the ways to tackle this problem is by tailoring process parameters through application of high laser power and base plate pre-heating. In this paper, a comparative study of optimum SLM fabrication conditions of Inconel 718 superalloy under high laser power and with and without plate pre-heating was conducted. Furthermore, the effect of layer thickness on melt pool characteristics, porosity and hardness were investigated to determine how laser power and pre-heating affect microstructure development.

Selection and Peer-review under responsibility of the scientific committee of the Materials Science: Composites, Alloys and Materials Chemistry.

1. Introduction

Additive manufacturing technologies over the past ten years have received a significant momentum in development. Every year there are more cases of their successful use in various industrial applications. Indeed, the unprecedented design flexibility, reduced lead time and material waste, are one the main advantages of additive technologies compared to traditional manufacturing routes, such as casting and forging. In some cases, it is even possible to achieve previously impossible results through the use of additive manufacturing technologies [1]. In particular, this applies to relatively small-scale production, where the timing of bringing finished products to the market and the ability to quickly change the range of products are important. For example, selective laser melting (SLM) is used in areas such as medicine and the aerospace industry, since complex shapes are especially required in these areas [2]. A huge number of scientific papers devoted to the study of the use of additive manufacturing technologies greatly contributes to their implementation in industry. A large number of works are devoted to the development of new materials for use in additive technologies [3–7]. After all, those materials, the use of which was difficult due to the significant segregations, cracking during processing, oxidation, and other reasons, have found application in additive technologies [8–10]. For example, refractory and other non-weldable materials [11–13].

However, the microstructure formation during selective laser melting is significantly different from traditional technologies [14]. These differences have recently opened up the possibility of developing tailored site-specific properties via control of process parameters and resulting microstructure [15,16]. Of the many types of nickel-based alloys, the attention of researchers is largely drawn to Inconel 718 alloy [17–20]. This alloy has a widespread use in gas turbines, space products, petrochemical and nuclear industries due to its excellent heat and corrosion resistance [21]. Inconel 718 alloy was previously used in studies devoted to the influence of SLM process parameters on the microstructure and properties. A set of various scanning strategies, laser spot diameters and parameters of laser radiation have been previously studied. In this work, unlike others, heating of the working zone (base plate) was used as an additional parameter to change the cooling conditions of the part and, as a result, the crystallization conditions.

Thus, the aim of this work was to determine the influence of SLM process parameters, such as high energy input, layer thickness and base plate preheating on the microstructure formation.

2. Experimental methods

As an initial material, a powder of the Inconel 718 heat-resistant nickel alloy obtained by gas atomization was used. The

* Corresponding author.
E-mail address: evgenii.borisov@icloud.com (E.V. Borisov).

https://doi.org/10.1016/j.matpr.2020.01.571
2214-7853/
Selection and Peer-review under responsibility of the scientific committee of the Materials Science: Composites, Alloys and Materials Chemistry.

particle size distribution was determined using the laser diffraction method on an Analysette 22 NanoTecPlus with a full scale range of 0.01–2000 μm. Investigations of the powder particles morphology were carried out using a scanning electron microscope TESCAN Mira 3 LMU (SEM) with an increase of 4–10^6-x with an accelerating voltage of 200 V–30 kV.

The samples were manufactured using the two selective laser melting machines. Specimens with 900 °C preheating were made at Aconity3D Midi (Aconity3D GmbH, Germany) machine, shown at Fig. 1(a). The machine is equipped with laser source with variable focal spot diameter, Gauss power distribution and a maximum power of 1000 W and is capable of up to 1200 °C preheating.

Specimens without preheating were manufactured at SLM 280HL (SLM Solutions GmbH, Germany) machine, equipped with two ytterbium fiber lasers with a power of 400 and 1000 W, with a laser scanning speed of up to 15 m/s. Compact rectangular samples were made in argon atmosphere using both machines.

Specific section cuts of YZ planes were used for optical examination on a Leica DMI 5000 light optical microscope in the magnification range from 50 to 1000 times. In order to reveal grain size and morphology, the specimens were etched in either glyceregia reagent (15 ml HCl, 10 ml glycerol and 5 ml HNO_3) or for preheated samples in acetic glyceregia (15 ml HCl; 10 ml acetic acid, 5 ml HNO_3; 0.5 ml glycerol). Porosity was estimated using the Archimedes method. To study the hardness of specimens a universal hardness tester ZwickRoell ZHU with 5 kg load was used.

XRD patterns were obtained using Bruker D8 diffractometer with CoKα radiation (λ = 1.79020 Å). Diffraction patterns were recorded within the 2θ range from 10° to 110° with a step size of 0.034°. The X-ray beam was collimated to a spot size of 3 mm in diameter on the sample surface.

3. Results and discussion

The powder of the Inconel 718 alloy used in this study has particle size in the range: d_{10} = 21.1 μm, d_{50} = 37.4 μm, d_{90} = 62 μm. Some of the particles have shown satellite outgrowths (Fig. 2a). The presence of such particles is typical for powders obtained with gas atomization. Investigations of the surface morphology of particles at high magnification showed that their surface has some irregularities, reflecting the cast microstructure with its cellular-dendritic crystallization (Fig. 2b).

Selective laser melting has many influencing parameters, such as the layer thickness, the power of the laser radiation and the distance between the individual laser scanning tracks (determined by the size of the laser spot), as well as the speed of the laser beam on the surface of the powder layer. Changes in these parameters

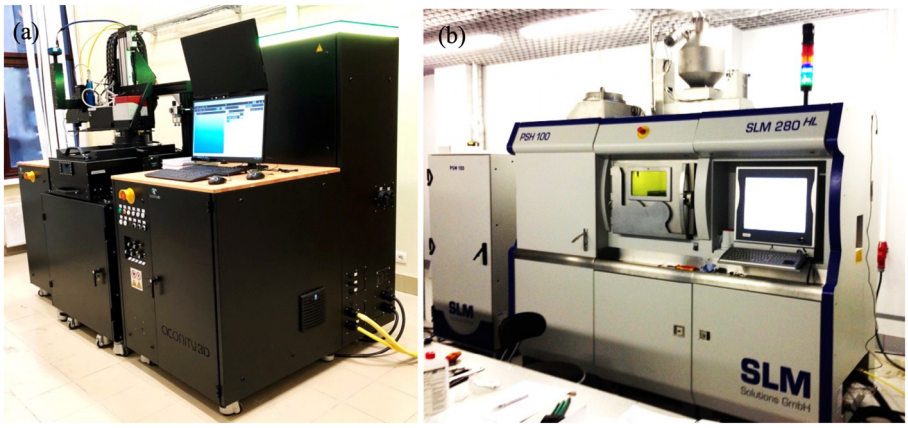

Fig. 1. Image of Aconity3D MIDI (a) and SLM 280HL (b) machines.

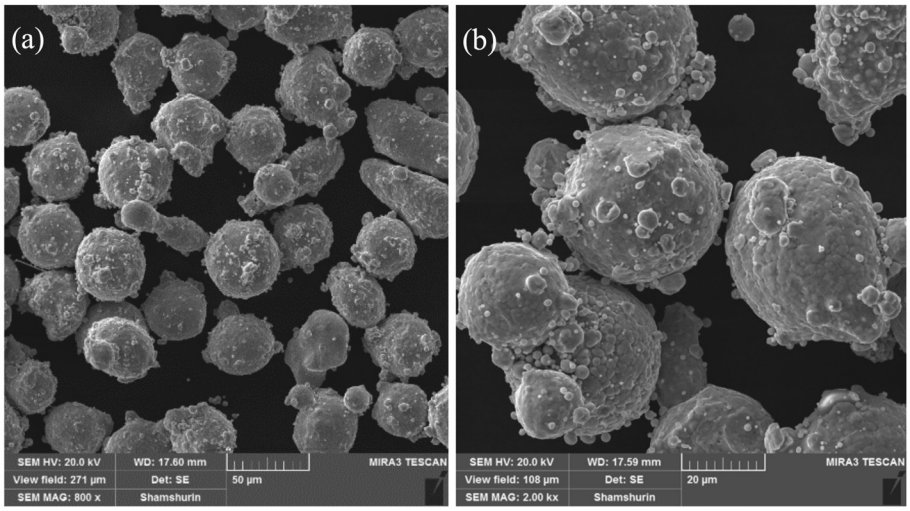

Fig. 2. SEM-images of Inconel 718 powder particles.

determine the thermal contribution to the material, the permeability of the powder layer, the depth of material heating, and the fusion of the new layer with the previous one. With the right choice of process parameters, it is possible to obtain preforms with densities close to 100%, but these parameters also affect the nature of crystallization processes occurring in the material. This leads to the formation of a different structure depending on the thermal fields generated using this combination of parameters.

In this study, SLM process with the same energy density at layer thicknesses of 50 and 100 μm, as well as with and without preheating was used to obtain the samples. The parameters were chosen in such a way as to ensure minimal porosity. For a layer with a thickness of 50 μm, laser focusing with a spot size of about 80 μm was used, and for a regime with a layer thickness of 100 μm, focusing with a spot size of about 700 μm was used. For the mode with preheating to 900 °C, the energy density is almost half that, which ensures the formation of solid material without pores. This is due to the lower energy required to melt the Inconel 718 alloy at elevated heating temperatures.

The microstructure of samples made using layers with a thickness of 50 μm without preheating the platform is shown in Fig. 3, as well as the microstructure samples made using layers with a thickness of 100 μm is shown in Fig. 4.

On the microstructure of the sample made using a small layer thickness, it is clearly seen that the melt pool has a width comparable in size to the depth, and the grains are fine without a preferred orientation. The formation of large elongated columnar grains in larger layers case (Fig. 4) is most likely caused by the differences in the geometry of the melt pool, which varies depending on the diameter of the laser spot. For samples of 50 μm layer height, the depth of penetration is almost equal to the diameter of the laser, which leads to the fact that the molten pool has a nearly equiaxial geometry (Fig. 3b).

Since the heat removal during the solidification of the metal occurs predominantly perpendicular to the interface between the liquid and solid phases, for the case of a layer thickness of 50 μm (Fig. 3), the direction of crystal growth differs substantially, which leads to the formation of multidirectional equiaxial grains. When using a regime with a layer thickness of 100 μm, the ratio of the laser spot diameter to the layer thickness is larger, therefore the resulting molten pool has a flatter profile, which is clearly seen in the image of the microstructure after etching (Fig. 4a).

Heat removal in the melt pool also goes perpendicular to the phase interface, but in this case it basically coincides with the building direction axis, which leads to the formation of grains elongated in the direction of growth due to epitaxial growth.

Applying preheating influences the thermal history of the material and therefore influence the microstructure of the parts. In the case of 900 °C pre-heating, the microstructure does not shown any traces of melt pool boundaries, likely owing to the formation of carbides (Fig. 5) and precipitation of Ni_3Nb phase (Fig. 6). As a result, the melt pool borders fade and a more uniform and coarsened microstructure, though still exhibiting visible elongated in build direction grains, appears (Fig. 5a and b).

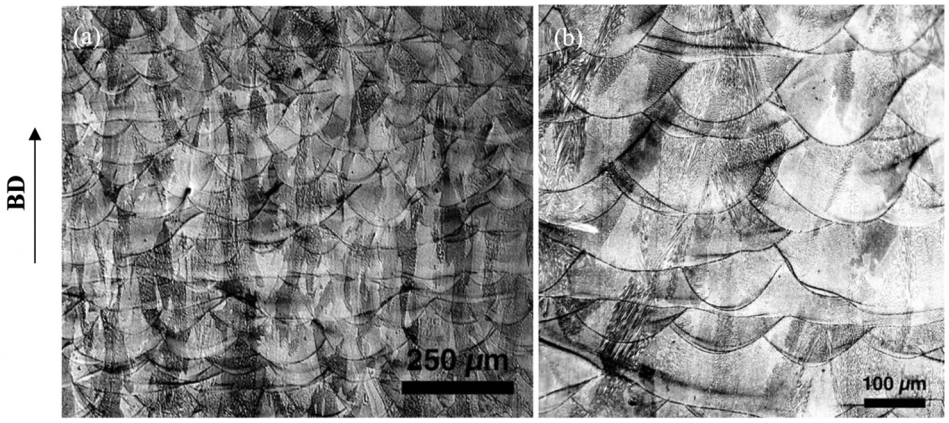

Fig. 3. Microstructure of specimens made by SLM with a layer thickness of 50 μm.

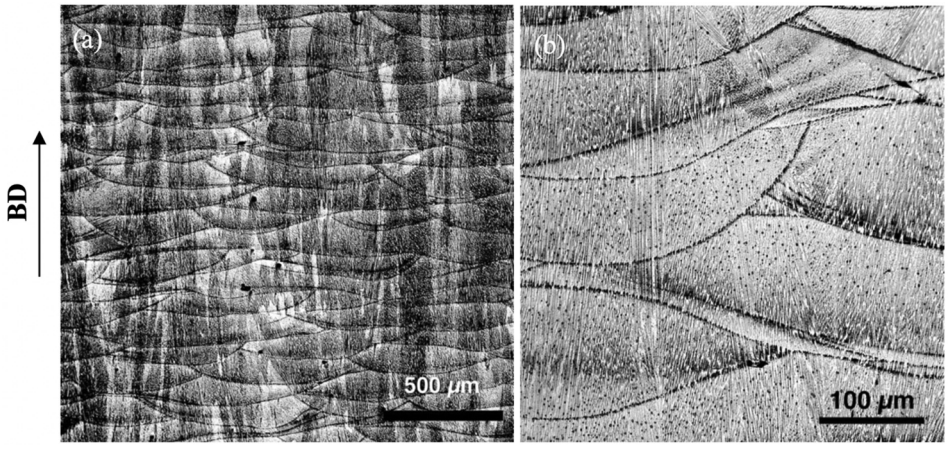

Fig. 4. Microstructure of specimens with a layer thickness of 100 μm and without pre-heating.

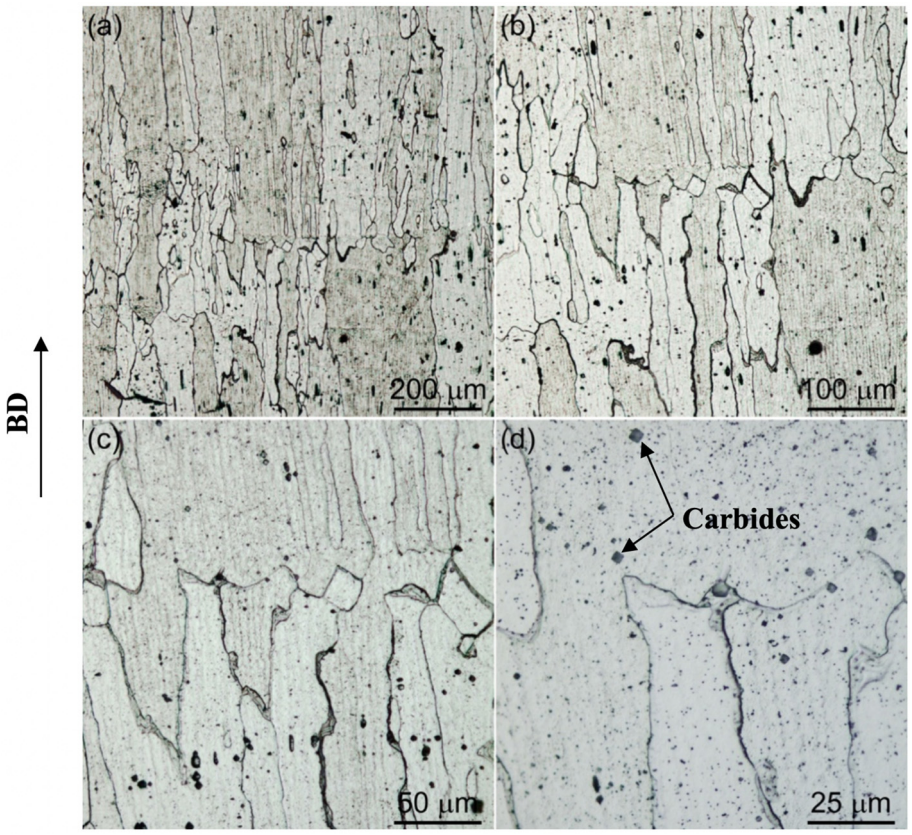

Fig. 5. Microstructure of specimen with a layer thickness of 100 μm and 900 °C preheating.

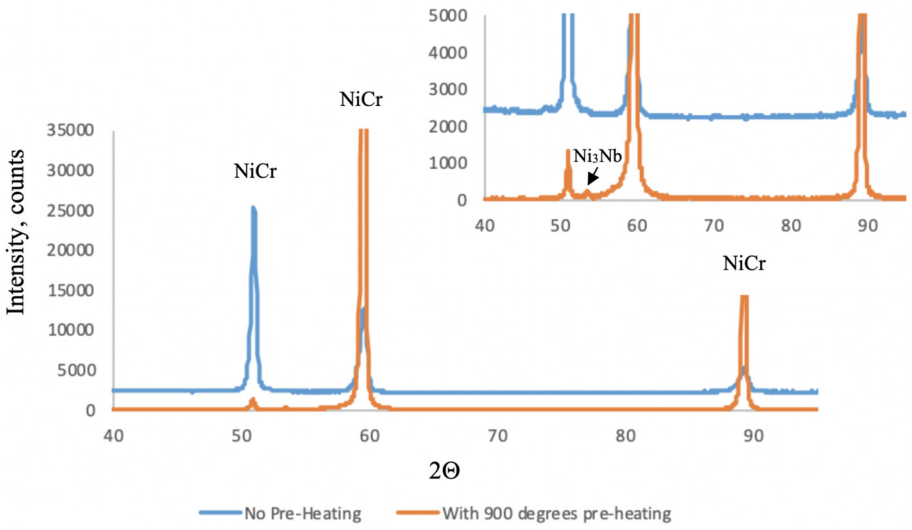

Fig. 6. XRD phase composition (including enlarged section), showing comparison between samples built with 100 μm layer thickness, with and without pre-heating.

The measurements showed that the average dendritic cell size at a layer thickness of 50 μm is 0.9–1.1 μm and at 100 μm is 1.3–2 μm (without preheating). In case of preheating, there were no visible dendritic cells found.

An increase in the heating temperature of the working area leads to a decrease in the intensity of the heat removal. This leads to the fact that the melt pool seems to solidify more slowly, resulting in reduced growth of crystals and loos of preferential texture (as seen in Fig. 6). In this case, more elongated grains (up to 4–5 mm long) are observed in the formed structure, in contrast to the case without preheating (with grain length up to 1.5–2 mm), which indicates an increase in the tendency to continue the growth of existed grains and a decrease in the formation of new ones. The formation of new grains disrupts the epitaxial growth of previously formed grains. If the new grain is well oriented along the direction of growth (in the case of Nickel alloys, this orientation is ⟨0 0 1⟩ along the direction of growth), its growth will continue. Otherwise, it will be displaced by the competitive growth of neighboring grains.

The results of hardness measurements of the samples are given in Table 1. The dependence of the hardness on the used regimes of sample production is clearly visible. In samples with a small grain

Table 1
Vickers hardness and porosity results.

Layer thickness, preheating	Hardness HV	Porosity, %
50 μm, without preheating	335 ± 10	0.11
100 μm, without preheating	287 ± 11	0.27
100 μm, with preheating	222 ± 8.5	0.15

size (made using the construction layer thickness of 590 μm), the hardness is greatest. Hence, with an increase in the layer thickness, and later on with the addition of preheating, the hardness value decreases, which is the result of microstructure coarsening. This is in good agreement with Hall-Petch law. Furthermore, it is shown that the addition of 900 °C pre-heating reduced the porosity and produces nearly dense (>99%) part.

4. Conclusion

This work presents studies on the influence of SLM process parameters, such as high energy input, layer thickness and base plate preheating on the microstructure formation, porosity and hardness of Inconel 718. It is shown that the presence of melt pool boundaries and dendritic structures is directly affected by the build layer thickness and pre-heating. In the case of a layer thickness of 50 μm and a small laser diameter, the orientation of the grains is substantially non-uniform, which leads to a small tendency to epitaxy and, as a result, to a small grain size in the final structure. In both cases, the layer thickness of 100 μm tendency to epitaxial growth was manifested to a significant degree, however, the use of preheating allowed to further lengthen the grain by changing the crystallization conditions. Furthermore, it was found that the melt pool characteristics are critical for the porosity development and hardness. It is shown that with pre-heating of 900 °C is possible to reduce both hardness and porosity of the build part.

Declaration of Competing Interest

The authors declare that they have no known competing financial interests or personal relationships that could have appeared to influence the work reported in this paper.

Acknowledgement

This research was supported by Russian Science Foundation grant (project No 19-79-30002).

References

[1] William E. Frazier, Metal additive manufacturing a review, J. Mater. Eng. Performance 23 (6) (2014) 1917–1928.
[2] Adrián Uriondo, Manuel Esperon-Miguez, Suresh Perinpanayagam, The present and future of additive manufacturing in the aerospace sector: a review of important aspects, Proc. Inst. Mech. Eng. G: J. Aeros. Eng. 229 (11) (2015) 2132–2147.
[3] P.A. Novikov, A.E. Kim, N.E. Ozerskoi, Q.S. Wang, A.A. Popovich, Plasma chemical synthesis of aluminum nitride nanopowder, Key Eng. Mater. 822 (2019) 628–633, https://doi.org/10.4028/www.scientific.net/KEM.822.628.
[4] T.Y. Makhmutov, N.G. Razumov, A.I. Shamshurin, Microstructure and mechanical properties of powder steel 16Cr – 2Ni – Mn – Mo obtained by mechanical alloying and spark plasma sintering, Key Eng. Mater. 822 (2019) 601–609, https://doi.org/10.4028/www.scientific.net/KEM.822.601.
[5] I.S. Goncharov, N.G. Razumov, A.I. Shamshurin, Q.S. Wang, Effect of the mechanical alloying and spark plasma sintering on microstructure, phase composition and chemical elements distribution of Nb-Si based composite, Key Eng. Mater. 822 (2019) 617–627, https://doi.org/10.4028/www.scientific.net/KEM.822.617.
[6] N.G. Razumov, A.A. Popovich, A.V. Grigor'ev, A.O. Silin, I.S. Goncharov, Morphology of high-strength heat-resistant steel powder for machines for additive production from shavings, Met. Sci. Heat Treat. 60 (2019) 710–714, https://doi.org/10.1007/s11041-019-00344-y.
[7] A.A. Popovich, N.G. Razumov, A.V. Grigoriev, A.V. Samokhin, V.S. Sufiiarov, I.S. Goncharov, A.A. Fadeev, M.A. Sinaiskii, Fabrication of the Nb–16Si alloy powder for additive technologies by mechanical alloying and spheroidization in electric-arc discharge thermal plasma, Russ. J. Non-Ferrous Met. 59 (2018) 671–676, https://doi.org/10.3103/S1067821218060160.
[8] N.G. Razumov, Q.S. Wang, A.A. Popovich, A.I. Shamshurin, Fabrication of spherical high-nitrogen stainless steel powder alloys by mechanical alloying and thermal plasma spheroidization, 2018: p. 020001. doi:10.1063/1.5030305.
[9] M.Yu. Maximov, A.S. Verevkin, A.A. Orlova, P.A. Novikov, A.O. Silin, O.V. Panchenko, A.A. Popovich, Studying of sintered WC-8Co powder with coatings of aluminum oxide produced by atomic layer deposition, J. Ceram. Process. Res. 18 (2) (2017) 103–107.
[10] D.V. Masaylo, A. Orlov, N.G. Razumov, A.A. Popovich, V. Popovich, Laser cladding of heat-resistant iron based alloy, Key Eng. Mater. 822 (2019) 520–525, https://doi.org/10.4028/www.scientific.net/KEM.822.520.
[11] I.S. Goncharov, L.V. Hisamova, L.Y. Saubanova, I.A. Polozov, Q.S. Wang, Synthesis of the in situ Nb-Si composites by binder jetting additive manufacturing technology, Key Eng. Mater. 822 (2019) 311–319, https://doi.org/10.4028/www.scientific.net/KEM.822.311.
[12] N.G. Razumov, A.A. Popovich, Q. Wang, Thermal plasma spheroidization of high-nitrogen stainless steel powder alloys synthesized by mechanical alloying, Met. Mater. Int. 24 (2018) 363–370, https://doi.org/10.1007/s12540-018-0040-8.
[13] S. Goncharov, N.G. Razumov, A.O. Silin, N.E. Ozerskoi, A.I. Shamshurin, A. Kim, Q.S. Wang, A.A. Popovich, Synthesis of Nb-based powder alloy by mechanical alloying and plasma spheroidization processes for additive manufacturing, Mater. Lett. (2019), https://doi.org/10.1016/J.MATLET.2019.03.014.
[14] V.A. Popovich, E.V. Borisov, V.S. Sufiyarov, et al., Tailoring the properties in functionally graded alloy Inconel 718 using additive technologies, Met. Sci. Heat Treat. 60 (2019) 701, https://doi.org/10.1007/s11041-019-00343-z.
[15] Popovich V.A., Borisov E.V., Heurtebise V., Riemslag T., Popovich A.A., Sufiiarov V.S., 2018. Creep and Thermomechanical Fatigue of Functionally Graded Inconel 718 Produced by Additive Manufacturing. In: & Materials Society T. (eds) TMS 2018 147th Annual Meeting & Exhibition Supplemental Proceedings. TMS 2018. The Minerals, Metals & Materials Series. Springer, Cham.
[16] T. Trosch, J. Strößner, R. Völkl, U. Glatzel, Microstructure and mechanical properties of selective laser melted Inconel 718 compared to forging and casting, Mater. Lett. 164 (2016) 428–431.
[17] V.Sh. Sufiiarov, A.A. Popovich, E.V. Borisov, I.A. Polozov, Selective laser melting of heat-resistant Ni-based alloy, Non-ferrous Metals 1 (2015) 32–35.
[18] Q. Jia, D. Gu, Selective laser melting additive manufacturing of Inconel 718 superalloy parts: densification, microstructure and properties, J. Alloys Compd. 585 (2014) 713–721.
[19] Xiaoqing Wang, Xibing Gong, Kevin Chou, Review on powder-bed laser additive manufacturing of Inconel 718 parts, Proc. Inst. Mech. Eng. B: J. Eng. Manuf. 231 (11) (2017) 1890–1903.
[20] I.I. Superalloys, High-temperature materials for aerospace and industrial plants (in Russian), Moscow: Metallurgy (1995) 385 p.
[21] M.J. Holzweissig, A. Taube, F. Brenne, M. Schaper, T. Niendorf, Microstructural characterization and mechanical performance of hot work tool steel processed by selective laser melting, Metall. Mater. Trans. B. 46 (2) (2015) 545–549.